Trilepton signature of minimal supergravity at the upgraded Fermilab Tevatron

V. Barger
Fermi National Accelerator Laboratory, P.O. Box 500, Batavia, Illinois 60510
and Department of Physics, University of Wisconsin, Madison, Wisconsin 53706

Chung Kao
Department of Physics, University of Wisconsin, Madison, Wisconsin 53706
(Received 30 November 1998; revised manuscript received 12 July 1999; published 11 November 1999)

The prospects for detecting trilepton events ($l=e$ or μ) from chargino-neutralino ($\chi_1^{\pm}\chi_2^0$) associated production are investigated for the upgraded Fermilab Tevatron Collider in the context of the minimal supergravity model (MSUGRA). In some regions of parameter space, $\chi_1^{\pm}$ and χ_2^0 decay dominantly into final states with τ leptons and the contributions from τ-leptonic decays enhance the trilepton signal substantially when soft cuts on lepton transverse momenta are used. Additional sources of the MSUGRA trilepton signal and dominant irreducible backgrounds are discussed. The dilepton (l^+l^-) invariant mass distribution near the end point is considered as a test of MSUGRA mass relations. Discovery contours for $p\bar{p}\rightarrow 3l+X$ at 2 TeV with an integrated luminosity of 2–30 fb^{-1} are presented in the MSUGRA parameter space of ($m_0, m_{1/2}$) for several choices of $\tan\beta$. [S0556-2821(99)07223-9]

PACS number(s): 12.60.Jv, 11.30.Er, 14.80.Ly

I. INTRODUCTION

In the near future the Main Injector (MI) of the Fermilab Tevatron Collider will run at 2 TeV center of mass energy with a luminosity of about 10^{32} cm^{-2} s^{-1} and will accumulate an integrated luminosity ($\mathcal{L}$) of 2 fb^{-1} (run II) or more at each of the Collider Detector at Fermilab (CDF) and the DØ detectors. It has been proposed to further upgrade the Tevatron luminosity to 10^{33} cm^{-2} s^{-1} to obtain a combined integrated luminosity $\mathcal{L}=30$ fb^{-1} (run III) [1,2]. Another possibility is that the MI will run at the run II luminosity for more years to accumulate a higher integrated luminosity. The order of magnitude increase in luminosity beyond the 0.1 fb^{-1} [3,4] now available will significantly improve the possibility that new physics beyond the standard model (SM) could be discovered before the CERN Large Hadron Collider (LHC) begins operation [2].

In this article we extend our recent study [5] on the prospects of detecting the trilepton signal with missing transverse energy in the minimal supergravity unified model (MSUGRA) at the upgraded Tevatron with a detailed consideration of backgrounds and optimized acceptance cuts to improve the trilepton search. The primary source of trileptons is the associated production of the lighter chargino ($\chi_1^{\pm}$) and the second lightest neutralino (χ_2^0) with both decaying to leptons [6–9]. In MSUGRA with gauge coupling unification, the sleptons ($\tilde{l}$), the lighter chargino ($\chi_1^{\pm}$) and the lighter neutralinos (χ_1^0, χ_2^0) are considerably less massive than the gluinos and squarks over most of the parameter space. Because of this, the trilepton signal ($3l+\not{E}_T$) is the most promising channel [3–9] for supersymmetric particle searches at the Tevatron. The trilepton background from SM processes can be greatly reduced with suitable cuts.

In supergravity unified models [10], supersymmetry (SUSY) is broken in a hidden sector with SUSY breaking communicated to the observable sector through gravitational interactions, leading naturally but not necessarily [11] to a common scalar mass (m_0), a common gaugino mass ($m_{1/2}$), a common trilinear coupling (A_0) and a bilinear coupling (B_0) at the grand unified scale ($M_{\rm GUT}$). Through minimization of the Higgs potential, the B coupling parameter of the superpotential and the magnitude of the Higgs mixing parameter μ are related to the ratio of Higgs-field vacuum expectation values (VEVs) ($\tan\beta\equiv v_2/v_1$) and to the mass of the Z boson (M_Z). The SUSY particle masses and couplings at the weak scale can be predicted by the evolution of renormalization group equations (RGEs) [12] from the unification scale [13,14]. We evaluate SUSY mass spectra and couplings in the minimal supergravity model in terms of m_0, $m_{1/2}$, A_0 and $\tan\beta$, along with the sign of the Higgs mixing parameter μ. The value of A_0 does not significantly affect our analysis; therefore, we take $A_0=0$ in our calculations. Non-universal boundary conditions among sfermion masses [15] or gaugino masses [16] could change the production cross section and branching fractions of the charginos and neutralinos. For $m_{1/2}=200$ GeV and $\tan\beta\lesssim 25$, a non-universality among sfermions significantly enhances the trilepton signal when 50 GeV $\lesssim m_0 \lesssim 130$ GeV [15].

The mass matrix of the charginos in the basis of the weak eigenstates ($\tilde{W}^{\pm}$, $\tilde{H}^{\pm}$) has the following form:

$$M_C=\begin{pmatrix} M_2 & \sqrt{2}M_W\sin\beta \\ \sqrt{2}M_W\cos\beta & \mu \end{pmatrix}. \qquad (1)$$

Since this mass matrix is not symmetric, its diagonalization requires two matrices [17]. The sign of the μ contribution in Eq. (1) establishes our sign convention[1] for μ, which is equivalent to the ISAJET convention [18].

[1]This sign convention for μ is opposite to that of Ref. [5].

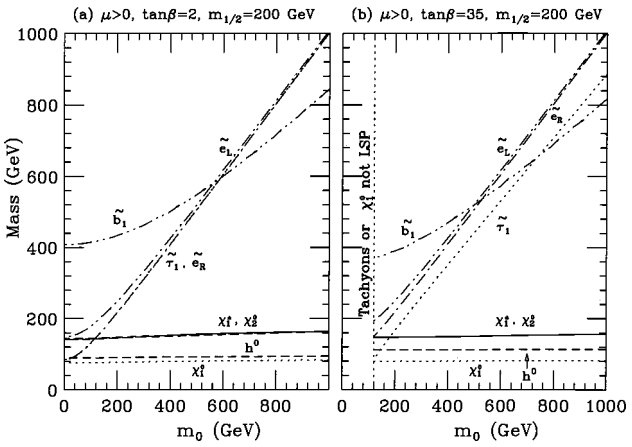

FIG. 1. Masses of χ_1^0, χ_2^0, $\chi_1^\pm$, $\tilde{e}_L$, $\tilde{e}_R$, $\tilde{\tau}_1$ and $\tilde{b}_1$ at the M_Z mass scale and mass of h^0 at the mass scale $Q=\sqrt{m_{\tilde{t}_L} m_{\tilde{t}_R}}$, versus m_0, with $M_{\rm SUSY}=1$ TeV, $m_{1/2}=200$ GeV and $\mu>0$ for (a) $\tan\beta=2$ and (b) $\tan\beta=35$. The shaded regions are excluded by theoretical requirements (tachyons and LSP).

In Fig. 1, we present the masses of the lightest neutralino (χ_1^0), the second lightest neutralino (χ_2^0), the lighter chargino $\chi_1^\pm$, the scalar electrons $\tilde{e}_L$ and $\tilde{e}_R$, the lighter tau slepton ($\tilde{\tau}_1$), and the lighter bottom squark $\tilde{b}_1$ at the mass scale of M_Z, and the mass of the lighter CP-even Higgs scalar (h^0) at the scale $Q=\sqrt{m_{\tilde{t}_L} m_{\tilde{t}_R}}$ [19,20], versus m_0, with $M_{\rm SUSY}=1$ TeV, $m_{1/2}=200$ GeV and $\mu>0$ for (a) $\tan\beta=2$ and (b) $\tan\beta=35$. To a good approximation, the mass of the lightest chargino, $m_{\chi_1^\pm}\sim m_{\chi_2^0}$, is about twice $m_{\chi_1^0}$. Also shown in Fig. 1 are the regions that do not satisfy the following theoretical requirements: tachyon free and the lightest neutralino as the lightest SUSY particle (LSP). There are several interesting aspects to note in Fig. 1:

(i) An increase in $\tan\beta$ leads to a larger m_h but a slight reduction in $m_{\chi_1^0}$, $m_{\chi_1^\pm}$, and a large reduction of $m_{\tilde{\tau}_1}$ and $m_{\tilde{b}_1}$.

(ii) Increasing m_0 raises the masses of scalar fermions.

(iii) In most of the MSUGRA parameter space, the weak-scale gaugino masses are related to the universal gaugino mass parameter $m_{1/2}$ by

$$m_{\chi_1^0}\sim 0.44 m_{1/2},$$
$$m_{\chi_1^\pm}\sim m_{\chi_2^0}\sim 0.84 m_{1/2}. \tag{2}$$

Consequently, the trilepton channel could provide valuable information about the value of $m_{1/2}$.

The masses of $\chi_1^\pm$ and χ_2^0 to the leading order in $M_W^2/(\mu^2-M_2^2)$ can be expressed as [21]

$$m_{\chi_1^\pm}=M_2-\frac{M_W^2(M_2+\mu\sin 2\beta)}{\mu^2-M_2^2+2M_W^2},$$
$$m_{\chi_2^0}=M_2-\frac{M_W^2(M_2+\mu\sin 2\beta)}{\mu^2-M_2^2}. \tag{3}$$

We find that M_2 and $|\mu|$ can be empirically expressed in GeV units as a function of the grand unified theory (GUT) scale masses $m_{1/2}$, m_0 and $\cos 2\beta$ as

$$M_2=0.851 m_{1/2}+0.00244 m_0-2.20,$$
$$|\mu|=a m_{1/2}+b\cos 2\beta+c,$$
$$a=2.34-0.153(m_0/100\ \text{GeV})+[1.10-0.141(m_0/100\ \text{GeV})]\cos 2\beta,$$
$$b=1.787 m_0-167.5,$$
$$c=1.909 m_0-178.7, \tag{4}$$

for 100 GeV $\lesssim m_0, m_{1/2} \lesssim 1000$ GeV and all $\tan\beta$ for which perturbative RGE solutions exist. These mass formulas hold to an accuracy of 5% for M_2, $m_{\chi_1^\pm}$ and $m_{\chi_2^0}$, and to an accuracy of 10% for $|\mu|$. These formulas provide useful approximations for quick estimates. In our analysis, we have used the numerical results from the RGEs.

The Yukawa couplings of the bottom quark (b) and the tau lepton (τ) are proportional to $\tan\beta$ and are thus greatly enhanced when $\tan\beta$ is large. In supersymmetric grand unified theories, the masses of the third generation sfermions are consequently very sensitive to the value of $\tan\beta$. As $\tan\beta$ increases, the lighter tau slepton ($\tilde{\tau}_1$) and the lighter bottom squark ($\tilde{b}_1$) become lighter than charginos and neutralinos while other sleptons and squarks remain heavy. Then, $\chi_1^\pm$ and χ_2^0 can dominantly decay into final states with tau leptons via real or virtual $\tilde{\tau}_1$.

One way to detect τ leptons is through their one-prong and three-prong hadronic decays. The CDF and the DØ collaborations are currently investigating the efficiencies for detecting these modes and for implementing a τ trigger [22]. It has been suggested that the τ leptons in the final state may be a promising way to search for $\chi_1^\pm\chi_2^0$ production at the Tevatron if excellent τ identification becomes feasible [9,23–25].

Another way of exploiting the τ signals [5], which we employ in this article, is to include the soft electrons and muons from leptonic τ decays by adopting softer but realistic p_T cuts on the leptons than conventionally used [7]. We find that this can improve the significance of the trilepton signal from $\chi_1^\pm\chi_2^0$ production [5].

After suitable cuts, there are two major sources of the SM background [5,7–9,24–28]: (i) $q\bar{q}\to W^*Z^*, W^*\gamma^*\to l\nu l\bar{l}$ or $l'\nu' l\bar{l}$ ($l=e$ or μ), with one or both gauge bosons being virtual,[2] and (ii) $q\bar{q}\to W^*Z^*, W^*\gamma^*\to l\nu\tau\bar{\tau}$ or $\tau\nu l\bar{l}$ and subsequent τ leptonic decays. In this article, we substantially improve the background calculations including effects from virtual W and Z and the contributions from virtual photons that are missing in ISAJET and not included in earlier studies.

[2]If it is not specified, W^* and Z^* represent real or virtual gauge bosons, while γ^* is a virtual photon.

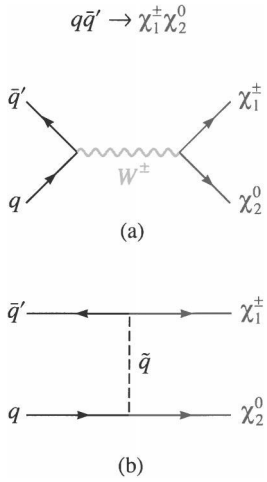

FIG. 2. Feynman diagrams of $q\bar{q}' \to \chi_1^{\pm}\chi_2^0$.

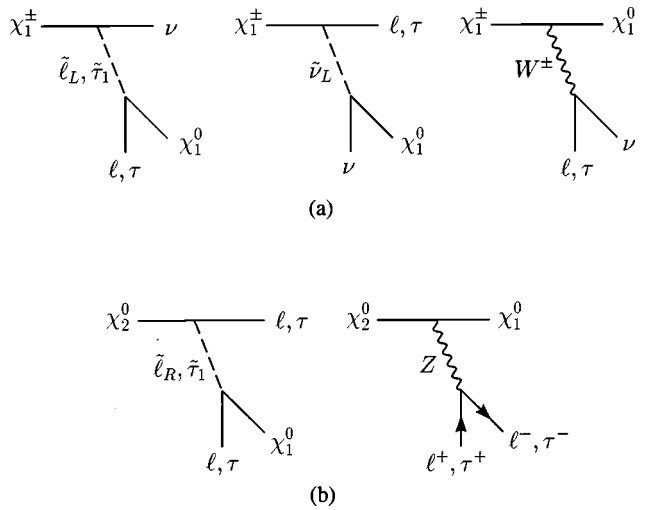

FIG. 3. Feynman diagrams of (a) $\chi_1^{\pm} \to l\nu\chi_1^0$ or $\tau\nu\chi_1^0$ and (b) $\chi_2^0 \to l^+l^-\chi_1^0$ or $\tau^+\tau^-\chi_1^0$.

These contributions are unexpectedly important. We reoptimize the acceptance cuts to reduce the larger background that resulted.

The experimental measurements of the $b \to s\gamma$ decay rate by the CLEO [29] and LEP Collaborations [30] place constraints on the parameter space of the minimal supergravity model [31]. It was found that $b \to s\gamma$ disfavors most of the MSUGRA parameter space when $\tan\beta \gtrsim 10$ and $\mu < 0$ [31]. Therefore, we concentrate on $\mu > 0$ in our analysis when $\tan\beta \gtrsim 10$.

In Sec. II we discuss the $p\bar{p} \to \chi_1^{\pm}\chi_2^0 + X$ cross section and the decay branching fractions of $\chi_1^{\pm}$ and χ_2^0. The acceptance cuts for the signal and background are discussed in Sec. III. We present the trilepton cross section from additional SUSY sources in Sec. IV. When the sleptons $(\tilde{l})$ and the sneutrinos $(\tilde{\nu})$ are light, they also contribute to the trilepton signal via production of $\tilde{l}\tilde{l}$ and $\tilde{l}\tilde{\nu}$. These contributions are at interesting levels when $m_0 \lesssim 150$ GeV and $\tan\beta \gtrsim 20$. The discovery potential of the trilepton search at the upgraded Tevatron is presented in Sec. V, with 3σ significance contours for observation or exclusion and 5σ significance contours for discovery. Section VI discusses the end point reconstruction at run III for invariant mass distribution of l^+l^- from the χ_2^0 decays. Our conclusions are given in Sec. VII.

II. ASSOCIATED PRODUCTION OF CHARGINO AND NEUTRALINO

In hadron collisions the associated production of the lighter chargino and the second lightest neutralino occurs via quark-antiquark annihilation in the s channel through a W boson $(q\bar{q}' \to W^{\pm} \to \chi_1^{\pm}\chi_2^0)$ and in the t and u channels through squark $(\tilde{q})$ exchanges. Figure 2 shows the Feynman diagrams of $q\bar{q}' \to \chi_1^{\pm}\chi_2^0$. The $p\bar{p} \to \chi_1^{\pm}\chi_2^0 + X$ cross section depends mainly on masses of the chargino $(m_{\chi_1^{\pm}})$ and the neutralino $(m_{\chi_2^0})$. For squarks much heavier than the gauge bosons, the s-channel W-resonance amplitude dominates. If the squarks are light, a destructive interference between the W boson and the squark exchange amplitudes can suppress the cross section by as much as 40%, compared to the s-channel contribution alone. For larger squark masses, the effect of negative interference is reduced.

Feynman diagrams of the chargino and neutralino decays into final states of leptons and neutrinos and the LSP are shown in Fig. 3: (a) $\chi_1^{\pm} \to l\nu\chi_1^0$ or $\tau\nu\chi_1^0$ and (b) $\chi_2^0 \to l^+l^-\chi_1^0$ or $\tau^+\tau^-\chi_1^0$. Figure 4 presents the branching fractions of χ_2^0 versus $\tan\beta$, with $m_{1/2} = 200$ GeV and several values of m_0 for both $\mu > 0$ and $\mu < 0$. For $\tan\beta \lesssim 5$, the branching fractions are sensitive to the sign of μ.

For $\mu > 0$, and $\tan\beta \sim 2$, we have found that the dominant decays are

$m_0 \lesssim 50$ GeV: $\chi_1^{\pm} \to \tilde{\nu}_L l$ and $\tilde{\tau}_1 \nu$,

$\chi_2^0 \to \tilde{l}_R l$, $\tilde{\tau}_1 \tau$ and $\tilde{\nu}_L \nu$;

60 GeV $\lesssim m_0 \lesssim$ 110 GeV:

$\chi_1^{\pm} \to \tilde{\tau}_1 \nu$,

$\chi_2^0 \to \tilde{l}_R l$ and $\tilde{\tau}_1 \tau$,

$(\chi_2^0 \to \tilde{\nu}_L \nu$ suppressed);

120 GeV $\lesssim m_0 \lesssim$ 170 GeV:

$\chi_1^{\pm}\chi_2^0 \to 3l + \not{E}_T$ via virtual $\tilde{l}$;

$m_0 \gtrsim 180$ GeV: $\chi_1^{\pm}$, $\chi_2^0 \to q\bar{q}\chi_1^0$.

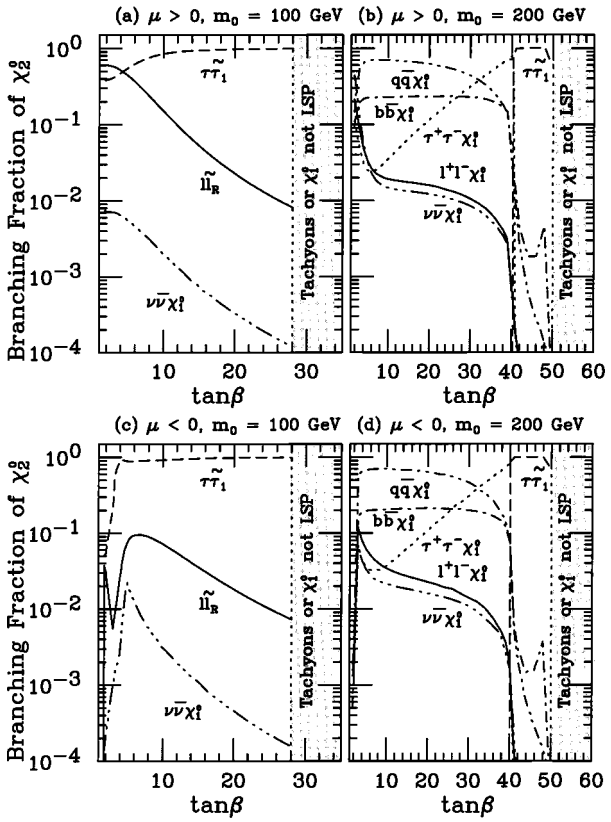

FIG. 4. Branching fractions of χ_2^0 decays into various channels versus $\tan\beta$ with $m_{1/2}=200$ GeV, for (a) $\mu>0$ and $m_0=100$ GeV, (b) $\mu>0$ and $m_0=200$ GeV, (c) $\mu<0$ and $m_0=100$ GeV, and (d) $\mu<0$ and $m_0=200$ GeV.

For $\mu<0$ and $\tan\beta\sim 2$, we have found that the dominant decays are

$$m_0 \lesssim 100 \text{ GeV}: \quad \chi_1^\pm \to \tilde{\nu}_L l, \qquad \chi_2^0 \to \tilde{\nu}_L \nu;$$

$$m_0 \gtrsim 110 \text{ GeV}: \quad \chi_1^\pm \to \tilde{\tau}_1 \nu, \qquad \chi_2^0 \to \chi_1^0 h^0.$$

For $m_0\sim 200$ GeV, χ_2^0 dominantly decays (i) into $\tau\bar{\tau}\chi_1^0$ for $25\lesssim\tan\beta\lesssim 40$, (ii) into $\tau\tilde{\tau}_1$ for $\tan\beta\gtrsim 40$. For $m_0\lesssim 300$ GeV and large $\tan\beta\gtrsim 35$, both $\tilde{\tau}_1$ and $\tilde{b}_1$ can be lighter than other sfermions, and $\chi_1^\pm$ and χ_2^0 can decay dominantly into final states with τ leptons or b quarks via virtual or real $\tilde{\tau}_1$ and $\tilde{b}_1$. For $m_0\gtrsim 400$ GeV and $5\lesssim\tan\beta\lesssim 40$, $B(\chi_2^0\to\tau^+\tau^-\chi_1^0)\sim B(\chi_2^0\to e^+e^-\chi_1^0)\sim 2\%$.

Figure 5 shows the cross section $\sigma(p\bar{p}\to\chi_1^\pm\chi_2^0\to 3l+X)$ at $\sqrt{s}=2$ TeV, which is the product $\sigma(p\bar{p}\to\chi_1^\pm\chi_2^0+X)\times B(\chi_1^\pm\to l\nu\chi_1^0)\times B(\chi_2^0\to l^+l^-\chi_1^0)$, versus $\tan\beta$ without acceptance cuts, with $m_{1/2}=200$ GeV and several values of m_0 for both $\mu>0$ and $\mu<0$. For $\tan\beta\lesssim 5$, the branching fractions are sensitive to the sign of μ. For $\mu<0$ and $\tan\beta\sim 2$, (a) with $m_0=100$ GeV, $B(\chi_2^0\to\tilde{\nu}\nu)=0.71$ and $B(\chi_2^0\to h^0\chi_1^0)=0.19$, some trileptons are due to $\chi_2^0\to\tilde{l}_R l$ and $\tilde{\tau}_1\tau$; (b) with $m_0=200$ GeV, $B(\chi_2^0\to h^0\chi_1^0)=0.99$ and consequently the trilepton rate drops sharply. For $m_0=100$ GeV and $m_{1/2}=200$ GeV, the curves end at $\tan\beta=28$, because the region with $\tan\beta\gtrsim 28$ is theoretically forbidden.

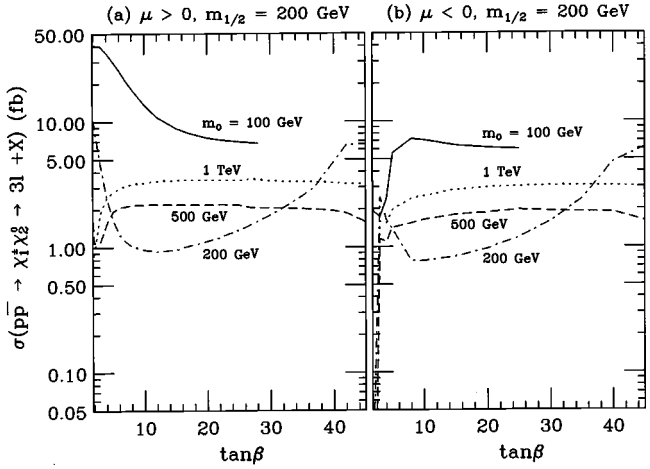

FIG. 5. Cross section of $p\bar{p}\to\chi_1^\pm\chi_2^0\to 3l+X$ at $\sqrt{s}=2$ TeV without cuts versus $\tan\beta$, with $m_{1/2}=200$ GeV and several values of m_0 for (a) $\mu>0$ and (b) $\mu<0$. For $m_0=100$ GeV, the curves end at $\tan\beta=28$, because the region with $\tan\beta\gtrsim 28$ is theoretically forbidden.

III. ACCEPTANCE CUTS

In this section we present results from simulations for the trilepton signal with an event generator and a simple calorimeter including our acceptance cuts. The ISAJET 7.40 event generator program [18] with the parton distribution functions of CTEQ3L [32] is employed to calculate the $3l+\not{E}_T$ signal from all possible sources of SUSY particles. A calorimeter with segmentation $\Delta\eta\times\Delta\phi=0.1\times(2\pi/24)$ extending to $|\eta|=4$ is used. We take an energy resolutions of $0.7/\sqrt{E}$ for the hadronic calorimeter and $0.15/\sqrt{E}$ for the electromagnetic calorimeter. Jets are defined to be hadron clusters with $E_T>15$ GeV in a cone with $\Delta R\equiv\sqrt{\Delta\eta^2+\Delta\phi^2}=0.7$. Leptons with $p_T>5$ GeV and within $|\eta_l|<2.5$ are considered to be isolated if the hadronic scalar E_T in a cone with $\Delta R=0.4$ about the lepton is smaller than 2 GeV.

The trilepton signal has dominant physics backgrounds from production of W^*V^*, V^*V^* ($V=Z$ or γ), and $t\bar{t}$. Most backgrounds from the SM processes can be removed with the following basic cuts:

(1) We require three isolated leptons in each event[3] with $p_T>5$ GeV and $|\eta_l|<2.0$ and a hadronic scalar E_T smaller than 2 GeV in a cone with $\Delta R=0.4$ around the lepton. This isolation cut removes background from $b\bar{b}$ and $c\bar{c}$ decays.

[3]The events with 4 isolated leptons are considered as 4-lepton signals in our analysis.

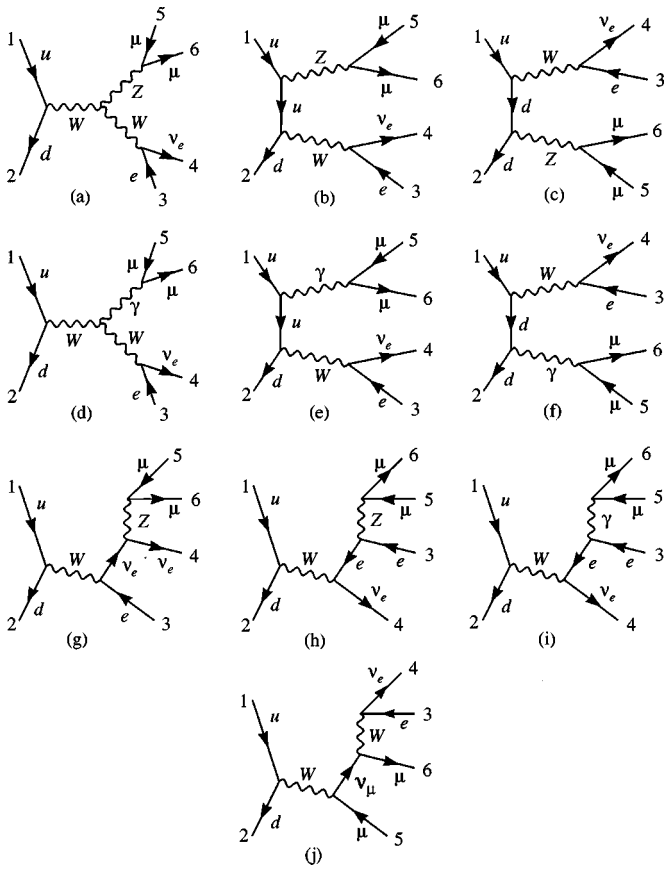

FIG. 6. Feynman diagrams of $u\bar{d}\to e^+\nu_e\mu^+\mu^-$.

(2) We require $\not{E}_T>25$ GeV in each event to remove backgrounds from SM processes such as Drell-Yan dilepton production, where an accompanying jet may fake a lepton.

(3) To reduce the background from W^*Z^* production, we require that the invariant mass of any opposite-sign dilepton pair with the same flavor not reconstruct the Z mass: $|M_{l\bar{l}}-M_Z|\geqslant 10$ GeV.

(4) To eliminate the background from J/ψ and Υ, and to reduce the background from $W^*\gamma^*$ production, we require a minimal value for the invariant mass of any opposite-sign dilepton pair with the same flavor: $M_{l\bar{l}}\geqslant 12$ GeV. A more severe $M_{l\bar{l}}$ cut is imposed later in Eq. (6).

Our acceptance cuts are chosen to be consistent with the experimental cuts proposed for run II [33,34] at the Tevatron as follows:

$$p_T(l_1)>11\ \text{GeV},$$

$$p_T(l_2)>7\ \text{GeV}\quad p_T(l_3)>5\ \text{GeV},$$

$$|\eta(l_1,l_2,l_3)|<2.0,$$

$$\not{E}_T>25\ \text{GeV},$$

$$M_{l\bar{l}}\geqslant 12\ \text{GeV}$$

$$|M_{l\bar{l}}-M_Z|\geqslant 10\ \text{GeV}, \qquad (5)$$

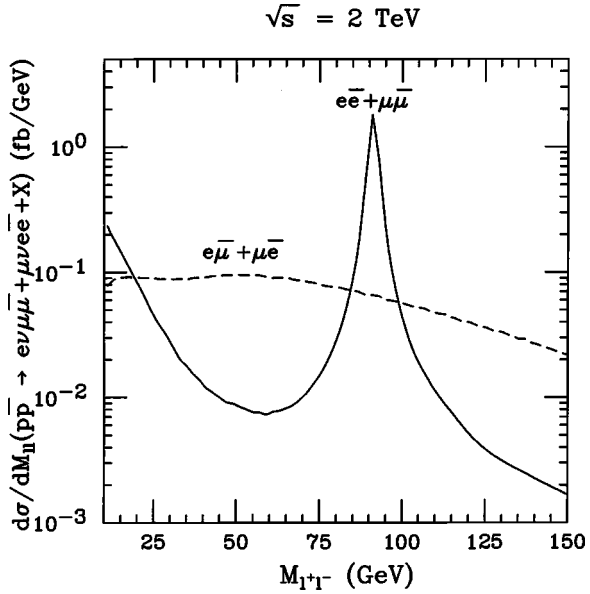

FIG. 7. Invariant mass ($M_{l\bar{l}}$) distribution of the lepton pairs with the same flavor and opposite sign [$d\sigma/dM_{l\bar{l}}(p\bar{p}\to e\nu\mu\bar{\mu}+\mu\nu e\bar{e}+X)$], for the dominant background from $q\bar{q}'\to l'\nu' l^+l^-$, at $\sqrt{s}=2$ TeV, with the basic cuts in Eq. (5), but without a Z veto. Also shown is the invariant mass distribution of $e\bar{\mu}+\mu\bar{e}$ with opposite signs.

and at least one lepton with $p_T(l)>11$ GeV and $|\eta(l)|<1.0$.

The surviving total background after these cuts has contributions from four major sources via quark anti-quark annihilation (Fig. 6): (i) production of $e^\pm\nu\mu^+\mu^-$ and $\mu^\pm\nu e^+e^-$ $(l'\nu' l\bar{l})$, (ii) production of $e^\pm\nu e^+e^-$ and $\mu^\pm\nu\mu^+\mu^-$ $(l\nu l\bar{l})$, (iii) production of $e^\pm\nu\tau^+\tau^-+\mu^\pm\nu\tau^+\tau^-$ $(l\nu\tau\bar{\tau})$, with subsequent τ leptonic decays, and (iv) production of $\tau^\pm\nu e^+e^-+\tau^\pm\nu\mu^+\mu^-$ $(\tau\nu l\bar{l})$, with subsequent τ leptonic decays. In addition, there are contributions from the production of $e\bar{e}\tau\bar{\tau}+\mu\bar{\mu}\tau\bar{\tau}$ $(l\bar{l}\tau\bar{\tau})$, with one τ decaying leptonically and another decaying hadronically. We employed the programs MADGRAPH [35] and HELAS [36] to evaluate the background cross section of $p\bar{p}\to 3l+\not{E}_T+X$ for contributions from all these five subprocesses. The background from $t\bar{t}$ was calculated with ISAJET.

We present invariant mass distribution of the same-flavor lepton pairs with opposite signs in Fig. 7 for the dominant background from $q\bar{q}'\to l'\nu' l\bar{l}$, with the basic cuts in Eq. (5), but without the Z veto. This background cross section from $W^*\gamma^*$ increases sharply as the invariant mass becomes smaller for $M_{l\bar{l}}\lesssim 30$ GeV. Therefore, a more stringent dilepton invariant mass cut than that in Eq. (5) is necessary to reduce the background from $W^*\gamma^*$.

Figure 8 shows the transverse mass $[M_T(l,\not{E}_T)]$ distribution of the lepton associated with two same-flavor and opposite-sign leptons, $d\sigma/dM_T(p\bar{p}\to e\nu\mu\bar{\mu}+\mu\nu e\bar{e}+X)$, from the dominant background $q\bar{q}'\to e\nu\mu\bar{\mu}+\mu\nu e\bar{e}$ at the upgraded Tevatron with the basic cuts in Eq. (5). Also shown

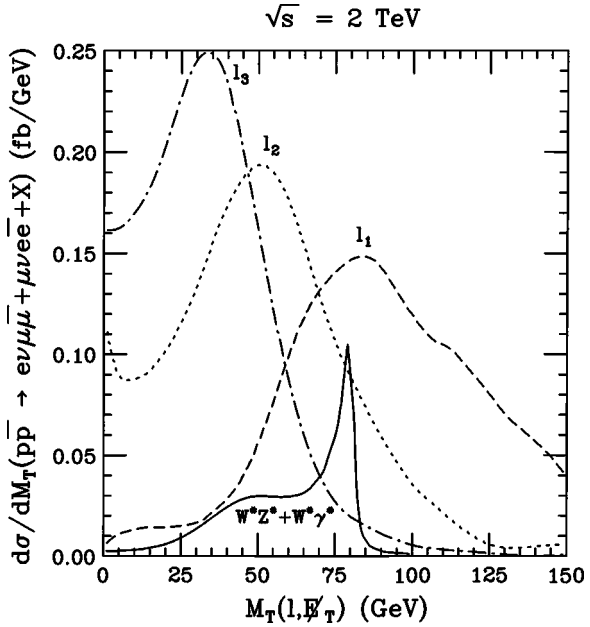

FIG. 8. Transverse mass $[M_T(l,\not{E}_T)]$ distribution of the lepton associated with two same-flavor and opposite-sign leptons from the dominant background $q\bar{q}' \to e\nu\mu\bar{\mu}+\mu\nu e\bar{e}$ with the basic cuts in Eq. (5). Also shown are the same distributions of trileptons $[p_T(l_1) \geq p_T(l_2) \geq p_T(l_3)]$ from the SUSY signal with the basic cuts for $\mu>0$, $\tan\beta=3$, $m_{1/2}=200$ GeV and $m_0=100$ GeV.

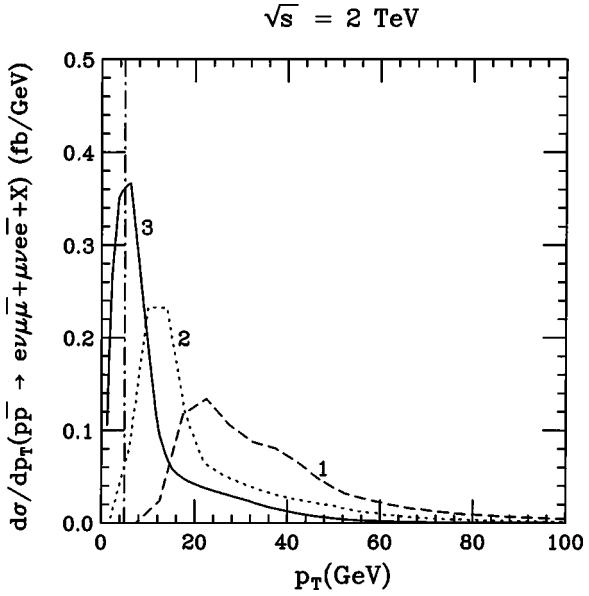

FIG. 9. Transverse momentum (p_T) distribution of the trileptons from $q\bar{q}' \to l'\nu l^+l^-$ at the upgraded Tevatron $[d\sigma/dp_T(p\bar{p} \to e\nu\mu\bar{\mu}+\mu\nu e\bar{e}+X)]$, with the basic cuts in Eq. (5), for the three leptons with $p_T(l_1) \geq p_T(l_2) \geq p_T(l_3) \geq 1$ GeV.

are the same distributions of trileptons $[p_T(l_1) \geq p_T(l_2) \geq p_T(l_3)]$ from the SUSY signal for $\mu>0$, $\tan\beta=3$, $m_{1/2}=200$ GeV and $m_0=100$ GeV with the basic cuts. This figure suggests that a cut on the transverse mass $[M_T(l,\not{E}_T)]$ around M_W can efficiently reduce the backgrounds from $W^*Z^*+W^*\gamma^*$.

To further reduce the background from W^*Z^* and $W^*\gamma^*$, we require that

$$|M_{l\bar{l}}-M_Z| \geq 15 \text{ GeV } (Z \text{ veto}),$$

$$M_{l\bar{l}} \geq 18 \text{ GeV } (\gamma \text{ veto}),$$

$$M_T(l',\not{E}_T) \leq 65 \text{ GeV or}$$

$$M_T(l',\not{E}_T) \geq 85 \text{ GeV } (W \text{ veto}). \quad (6)$$

where $M_{l\bar{l}}$ is the invariant mass for any pair of leptons with the same flavor and opposite signs, and $M_T(l',\not{E}_T)$ is the transverse mass of the lepton associated with $l\bar{l}$.

Some $3l$ events could be due to $Z+$jets and $W+$jets. Since these sources always originate from $b \to cl\nu$ followed by $c \to sl\nu$, they can be removed by imposing an angular separation cut between the isolated leptons, giving a background consistent with zero. This angular separation cut causes almost no signal loss.

The transverse momentum (p_T) distribution for the three leptons of the dominant background is shown in Fig. 9 for $p\bar{p} \to e\nu\mu\bar{\mu}+\mu\nu e\bar{e}+X$. We label the trileptons as $l_{1,2,3}$, where $l=e$ or μ, according to the ordering $p_T(l_1)>p_T(l_2)>p_T(l_3)$ of their transverse momenta. Figure 10 presents the transverse momentum distribution of the three leptons from the SUSY signal with $\mu>0$, $\tan\beta=10$, $m_{1/2}=200$ GeV and $m_0=100$ GeV. The most important lesson we learn from Fig. 10 is that a large number of l_3's from the SUSY particle decays have a p_T less than 5 GeV. Therefore, it is very important to have a soft p_T acceptance cut on l_3 to retain the trilepton events from SUSY sources [5].

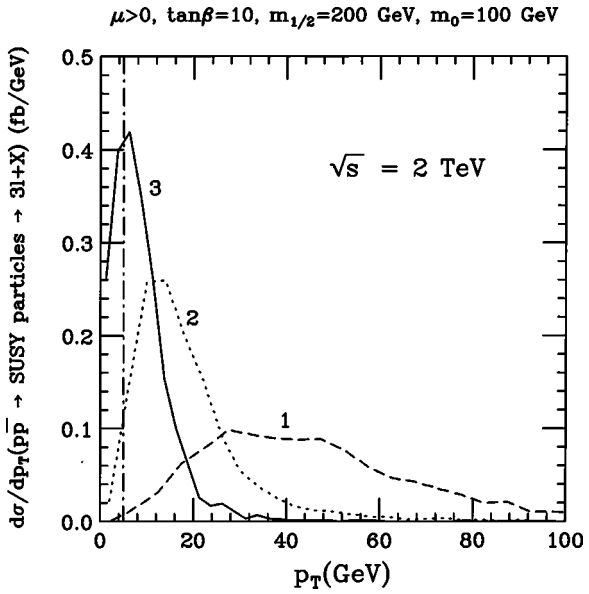

FIG. 10. Transverse momentum distribution of $p\bar{p} \to$ SUSY particles $\to 3l+X$ at $\sqrt{s}=2$ TeV with the basic cuts in Eq. (5) and $p_T(l_1) \geq p_T(l_2) \geq p_T(l_3) \geq 1$ GeV, for $\mu>0$, $\tan\beta=10$, $m_{1/2}=200$ GeV and $m_0=100$ GeV

TABLE I. The cross section of $p\bar{p}\to$SUSY particles$\to 3l+X$ in fb versus $\tan\beta$ for $m_{1/2}=200$ GeV and $m_0=100$ GeV along with the trilepton cross sections of the SM backgrounds (BG) and values of statistical significance ($N_S\equiv S/\sqrt{B}$, $S=$ number of signal events, and $B=$ number of background events) for an integrated luminosity of $\mathcal{L}=30$ fb^{-1}, at the upgraded Tevatron with four sets of cuts: (a) basic cuts: cuts in Eq. (5); (b) soft cuts A: cuts in Eqs. (5) and (6); (c) soft cuts B: the same cuts as soft cuts A, except requiring 18 GeV $\leqslant M_{ll}\leqslant 75$ GeV; (d) hard cuts: the same cuts as soft cuts A, except requiring $M_{ll}\geqslant 12$ GeV, and $p_T(l_1,l_2,l_3)>20$, 15, and 10 GeV.

$\tan\beta\setminus$ cuts	Basic	Soft A	Soft B	Hard
3	12.8	8.82	8.41	4.04
10	3.49	2.57	2.43	1.13
20	1.18	0.90	0.79	0.34
25	0.66	0.50	0.43	0.20
SM BG				
$l'\nu' l\bar{l}$	2.63	0.72	0.60	0.32
$l\nu l\bar{l}$	2.09	0.41	0.30	0.20
$l\nu\tau\bar{\tau}$	0.60	0.45	0.41	0.22
$\tau\nu l\bar{l}$	0.37	0.20	0.13	0.11
$ll\tau\bar{\tau}$	0.12	0.08	0.06	0.04
$t\bar{t}$	0.14	0.11	0.06	0.009
Total BG	5.95	1.97	1.56	0.90
$\tan\beta\backslash N_S$				
3	28.7	34.4	36.9	23.3
10	7.8	10.0	10.7	6.5
20	2.6	3.5	3.5	2.0
25	1.5	1.9	1.9	1.2

The effects of acceptance cuts on the signal and background are demonstrated in Table I. The trileptons are due to $\chi_1^\pm\chi_2^0$ production and the additional SUSY particle sources that are discussed in the next section. The cross sections of the signal with $m_{1/2}=200$ GeV, $m_0=100$ GeV, and several values of $\tan\beta$, along with $l\nu l\bar{l}$, $t\bar{t}$ and ZZ backgrounds are presented for four sets of cuts: (a) basic cuts: acceptance cuts in Eq. (5); (b) soft cuts A: acceptance cuts in Eqs. (5) and (6); (c) soft cuts B: the same cuts as soft cuts A, except requiring 18 GeV $\leqslant M_{ll}\leqslant 75$ GeV; (d) hard cuts: the same cuts as soft cuts A, except requiring $M_{ll}\geqslant 12$ GeV and $p_T(l_1,l_2,l_3)>20$, 15, and 10 GeV. We observe that the soft cuts can considerably enhance the signal significance. A more strict cut to require $M_{ll}<75$ GeV as in soft cuts B can further reduce the backgrounds from $l'\nu' l\bar{l}$ as well as $l\nu l\bar{l}$ with a slight reduction in the trilepton signal for most SUGRA parameters and might slightly improve the statistical significance. The reach with each of the soft cuts is qualitatively similar. For brevity, we will present results with soft cuts A in this article.

In Table II, we present masses of relevant SUSY particles for four sets of MSUGRA parameters[4]: The trilepton signal cross sections and values of statistical significance for these sets of parameters are presented in Table III with an integrated luminosity of $\mathcal{L}=30$ fb^{-1}.

TABLE II. Masses of relevant SUSY particles for four MSUGRA cases along with the value of the Higgs mixing parameter $\mu>0$.

Parameters \ cases	I	II	III	IV
m_0	100	140	200	250
$m_{1/2}$	200	175	140	150
A_0	0	0	−500	−600
$\tan\beta$	3	35	35	3
Masses of relevant SUSY particles				
The μ parameter	312	241	286	369
$m_{\tilde{g}}$	508	455	375	403
$m_{\tilde{u}_L}$	457	417	375	420
$m_{\tilde{d}_L}$	463	424	383	426
$m_{\tilde{u}_R}\sim m_{\tilde{d}_R}$	440	406	367	413
$m_{\tilde{t}_1}$	306	297	153	134
$m_{\tilde{b}_1}$	418	329	213	346
$m_{\chi_1^\pm}$	141	126	106	109
$m_{\chi_1^0}$	76	69	56	57
$m_{\chi_2^0}$	143	127	107	111
$m_{\tilde{l}_R}$	133	162	212	260
$m_{\tilde{\tau}_1}$	132	104	88	257
$m_{\tilde{l}_L}$	180	194	229	275
$m_{\tilde{\nu}_L}$	165	177	214	266

Case I: In this case, $m_{\tilde{l}_R}\sim m_{\tilde{\tau}_1}<m_{\chi_1^\pm}\sim m_{\chi_2^0}$, $B(\chi_2^0\to\tilde{l}_R l)=58\%$, $B(\chi_2^0\to\tilde{\tau}_1\tau)=41\%$, and $B(\chi_1^\pm\to\tilde{\tau}_1\nu)=49\%$, so a large rate for trilepton events is expected. The $\chi_1^\pm\chi_2^0$ production contributes about 81% of the total trilepton signal. The MSUGRA parameters for this case are in the cosmologically favored region of parameter space with an appropriate χ_1^0 relic density for cold dark matter ($\Omega_{\chi_1^0}h^2=0.24$) [20,38].

Case II: This parameter space point has a large value of $\tan\beta=35$ and $\tilde{\tau}_1$ is much lighter than $\chi_1^\pm$ and χ_2^0; $B(\chi_2^0\to\tilde{\tau}_1\tau)\sim 100\%$, and $B(\chi_1^\pm\to\tilde{\tau}_1\nu)\sim 100\%$. Here, we anticipate that an inclusive trilepton signal can be extracted with relatively soft lepton p_T cuts, since the detected leptons typically come from τ decays.

Case III: This parameter space point also has a large $\tan\beta$, but the A_0 parameter is chosen so that relatively light $\tilde{t}_1$, $\tilde{b}_1$ and $\tilde{\tau}_1$ are generated; $B(\chi_2^0\to\tilde{\tau}_1\tau)\sim 100\%$, and $B(\chi_1^\pm\to\tilde{\tau}_1\nu)\sim 100\%$. The trileptons should occur at a similar rate as in case II. The rather large $\tilde{t}_1\tilde{t}_1$ production cross section may yield an observable $\tilde{t}_1$ signal.

Case IV: This parameter space choice has a small value of $\tan\beta=3$ and the A_0 has been chosen such that $\tilde{t}_1$ is light,

[4]These cases were selected for the SUGRA study in the RUN II Workshop on Supersymmetry/Higgs at the Fermilab [37].

TABLE III. The cross section (in fb) of $p\bar{p}\to$SUSY particles$\to 3l+X$ at $\sqrt{s}=2$ TeV for the four MSUGRA cases described in Table II with contributions from various SUSY channels. For each MSUGRA case, the statistical significance $N_S\equiv S/\sqrt{B}$, $S(B)=$ number of signal (background) events, is presented for an integrated luminosity $\mathcal{L}=30$ fb^{-1} and the four sets of acceptance cuts described in Table I.

Acceptance cuts \ cases	I	II	III	IV	SM background
Cross section					
Basic cuts	12.8	1.58	1.94	4.13	5.95
Soft cuts A	8.82	1.21	1.32	3.06	1.97
Soft cuts B	8.41	0.97	1.18	2.97	1.56
Hard cuts	4.04	0.47	0.30	1.58	0.90
Statistical significance: $N_S\equiv S/\sqrt{B}$					
Basic cuts	28.7	3.5	4.4	9.3	
Soft cuts A	34.4	4.7	5.2	12.0	
Soft cuts B	36.9	4.3	5.2	13.0	
Hard cuts	23.3	2.7	1.7	8.8	

while both l_R and $\tilde{\tau}_1$ are heavier than $\chi^{\pm}$; $B(\chi_2^0\to\chi_1^0 e\bar{e}+\chi_1^0\mu\bar{\mu})=6.6\%$, and $B(\chi_1^{\pm}\to e\nu+\mu\nu)=23\%$. This case could also provide an opportunity to search for $\tilde{t}_1\tilde{t}_1$ production where $\tilde{t}_1\to b\chi_1^{\pm}$ with $\chi_1^{\pm}\to l\nu_l\chi_1^0$.

Most trileptons in cases I and IV have higher p_T than those in cases II and III, because the latter contain some secondary leptons from τ decays.

At run II with 2 fb^{-1} integrated luminosity, we expect about 4 events per experiment from the background cross section of 1.97 fb. Then the signal cross section must yield a minimum of 6 signal events for discovery; the Poisson probability for the SM background to fluctuate to this level is less than 0.8%. At run III with $\mathcal{L}=30$ fb^{-1}, we would expect about 59 background events; a 5σ signal would be 38 events corresponding to a signal cross section of 1.28 fb, and a 3σ signal would be 23 events corresponding to a signal cross section of 0.77 fb.

IV. ADDITIONAL SOURCES OF TRILEPTONS

In addition to the associated production of $\chi_1^{\pm}\chi_2^0$, there are other SUSY contributions to trilepton events.

(1) If the sleptons and sneutrinos are light, $\tilde{l}\tilde{\nu}$ and $\tilde{l}\tilde{l}$ can make an important contribution to the trilepton signal and $\tilde{\nu}\tilde{\nu}$ can make a small contribution.

(2) When the charginos ($\chi_{1,2}^{\pm}$), and the neutralinos ($\chi_{2,3,4}^0$) are not too heavy, they contribute to the trileptons via $\chi_2^0\chi_2^0$, $\chi_2^0\chi_3^0$, $\chi_3^0\chi_4^0$, $\chi_1^{\pm}\chi_3^0$, $\chi_2^{\pm}\chi_3^0$, and $\chi_2^{\pm}\chi_4^0$ production.

(3) When the gluino ($\tilde{g}$), the squarks ($\tilde{q}$), and the neutralinos ($\chi_{2,3,4}^0$) are not too heavy, they also contribute to the trileptons via the production of $\tilde{g}\chi_{2,3}^0$ and $\tilde{q}\chi_{2,3}^0$.

(4) The production of $\tilde{g}\tilde{g}$ and $\tilde{q}\tilde{q}$ also make small trilepton contributions.

For $m_0\gtrsim 500$ GeV and $m_{1/2}\lesssim 300$ GeV, the associated production of $\chi_1^{\pm}\chi_2^0$, contributes at least 95% of the trilepton signal. For $m_0\lesssim 150$ and $\tan\beta\gtrsim 20$, production of $\tilde{l}\tilde{\nu}$ and $\tilde{l}\tilde{l}$ can enhance the trilepton cross section and may yield observable signals at run III. We summarize the contributions to trileptons from various relevant channels for $\mu>0$ in Table IV and for $\mu<0$ in Table V.

TABLE IV. The cross section of $p\bar{p}\to 3l+X$ in fb versus $\tan\beta$ with contributions from various relevant SUSY channels at $\sqrt{s}=2$ TeV with the acceptance cuts described in Eqs. (5) and (6) for $\mu>0$, $m_{1/2}=200$ GeV, $\tan\beta=2$, 10, 20 and 35 (25 for $m_0=100$ GeV).

Channel \ $\tan\beta$	2	10	20	35(25)
(i) $m_0=100$ GeV				
Total	9.58	2.57	0.90	0.50
$\chi_1^{\pm}\chi_2^0$	7.86	1.74	0.40	0.13
$\tilde{l}\tilde{\nu}$	0.68	0.32	0.18	0.10
$\tilde{l}\tilde{l}$	0.35	0.16	0.15	0.13
$\chi_2^0\chi_2^0$, $\chi_2^0\chi_3^0$, $\chi_3^0\chi_4^0$,	0.30	0.12	0.05	0.05
$\chi_1^{\pm}\chi_{3,4}^0$, $\chi_2^{\pm}\chi_{3,4}^0$ $\chi_1^{\pm}\chi_2^{\mp}$, $\chi_2^{\pm}\chi_2^{\mp}$	0.04	0.08	0.06	0.05
$\tilde{g}\chi_{2,3}^0$, $\tilde{q}\chi_{2,3}^0$, $\tilde{g}\tilde{g}$, $\tilde{q}\tilde{q}$, $\tilde{\nu}\tilde{\nu}$	0.35	0.15	0.06	0.04
(ii) $m_0=200$ GeV				
Total	2.11	0.23	0.25	0.31
$\chi_1^{\pm}\chi_2^0$	1.92	0.16	0.17	0.19
$\tilde{l}\tilde{\nu}$	0.06	0.02	0.02	0.03
$\tilde{l}\tilde{l}$	0.03	–	0.01	0.01
$\chi_2^0\chi_2^0$, $\chi_2^0\chi_3^0$, $\chi_3^0\chi_4^0$,	0.02	–	0.01	0.02
$\chi_1^{\pm}\chi_{3,4}^0$, $\chi_2^{\pm}\chi_{3,4}^0$ $\chi_1^{\pm}\chi_2^{\mp}$, $\chi_2^{\pm}\chi_2^{\mp}$	0.01	0.02	0.02	0.02
$\tilde{g}\chi_{2,3}^0$, $\tilde{q}\chi_{2,3}^0$, $\tilde{g}\tilde{g}$, $\tilde{q}\tilde{q}$, $\tilde{\nu}\tilde{\nu}$	0.07	0.03	0.02	0.04
(iii) $m_0=500$ GeV				
Total	0.27	0.48	0.46	0.42
$\chi_1^{\pm}\chi_2^0$	0.26	0.46	0.45	0.41
$\chi_2^0\chi_2^0$, $\chi_2^0\chi_3^0$, $\chi_3^0\chi_4^0$,	–	0.01	–	–
$\chi_1^{\pm}\chi_{3,4}^0$, $\chi_2^{\pm}\chi_{3,4}^0$ $\chi_1^{\pm}\chi_2^{\mp}$, $\chi_2^{\pm}\chi_2^{\mp}$	0.01	0.01	0.01	0.01
$\tilde{g}\chi_{2,3}^0$, $\tilde{q}\chi_{2,3}^0$, $\tilde{g}\tilde{g}$, $\tilde{q}\tilde{q}$, $\tilde{\nu}\tilde{\nu}$	–	–	–	–

TABLE V. The cross section (in fb) of $p\bar{p}\to 3l+X$ at $\sqrt{s}=2$ TeV with contributions from various SUSY channels and the acceptance cuts described in Eqs. (5) and (6), for $\mu<0$, $m_{1/2}=160$ GeV, $\tan\beta=2$ and several choices of m_0.

Channel \ m_0 (GeV)	100	200	500	1000
Total	4.91	3.24	1.12	0.89
$\chi_1^\pm\chi_2^0$	3.74	2.62	1.07	0.88
$\tilde{l}\tilde{\nu}$	0.12	0.15	–	–
$\tilde{l}\tilde{l}$	0.12	0.03	–	–
$\chi_2^0\chi_2^0$, $\chi_2^0\chi_3^0$, $\chi_3^0\chi_4^0$,	0.20	0.09	0.01	–
$\chi_1^\pm\chi_{3,4}^0$, $\chi_2^\pm\chi_{3,4}^0$ $\chi_1^\pm\chi_2^\mp$, $\chi_2^\pm\chi_2^\mp$	0.04	0.02	–	–
$\tilde{g}\chi_{2,3}^0$, $\tilde{q}\chi_{2,3}^0$,$\tilde{g}\tilde{g}$, $\tilde{q}\tilde{q}$,$\tilde{\nu}\tilde{\nu}$	0.69	0.32	0.04	0.01

V. DISCOVERY POTENTIAL AT THE TEVATRON

The cross sections for the trilepton signal after cuts are shown in Fig. 11 versus $m_{1/2}$ with $\tan\beta=3$ and several values of m_0 for both $\mu>0$ and $\mu<0$. Figure 12 shows the cross sections of the trilepton signal and background after cuts versus $m_{1/2}$ with several values of m_0 and $\mu>0$ for $\tan\beta=10$ and $\tan\beta=35$. Also shown are lines for (i) 6 signal events with $\mathcal{L}=2$ fb^{-1} and (ii) a 5σ signal as well as a 3σ signal with $\mathcal{L}=30$ fb^{-1}.

To assess the overall discovery potential of the upgraded Tevatron, we present the 99% C.L. observation contour at run II and the 5σ discovery contour as well as the 3σ observation contour at run III in Fig. 13 for $p\bar{p}\to$SUSY particles$\to 3l+X$ at $\sqrt{s}=2$ TeV, with soft acceptance cuts [Eqs. (5) and (6)], in the parameter space of $(m_0,m_{1/2})$, with $\tan\beta=2$, for (a) $\mu>0$ and (b) $\mu<0$. All

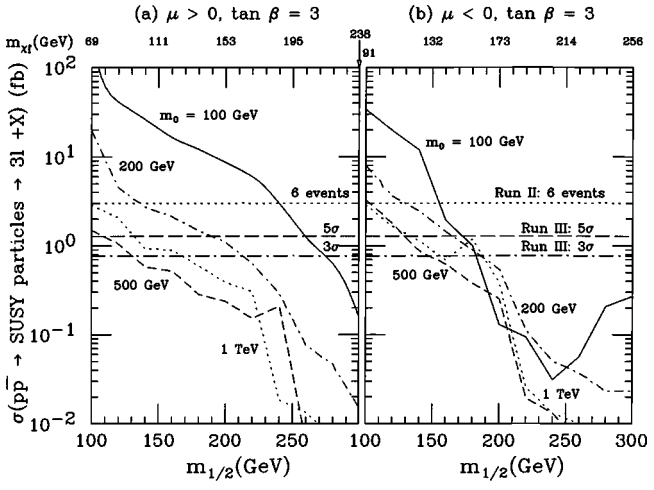

FIG. 11. Cross section of $p\bar{p}\to$SUSY particles$\to 3l+X$ with soft acceptance cuts [Eqs. (5) and (6)], versus $m_{1/2}$, at $\sqrt{s}=2$ TeV, with $\tan\beta=2$, $m_0=100$ GeV (solid line), 200 GeV (dot-dashed line), 500 GeV (dashed line) and 1000 GeV (dotted line) for (a) $\mu>0$ and (b) $\mu<0$. Also noted by lines are the cross sections for (i) 6 signal events with $\mathcal{L}=2$ fb^{-1} (dotted line) and (ii) 5σ signal (dashed line) as well as 3σ signal (dot-dashed line) for $\mathcal{L}=30$ fb^{-1}. The chargino mass is given on the top horizontal scale with $m_0=500$ GeV.

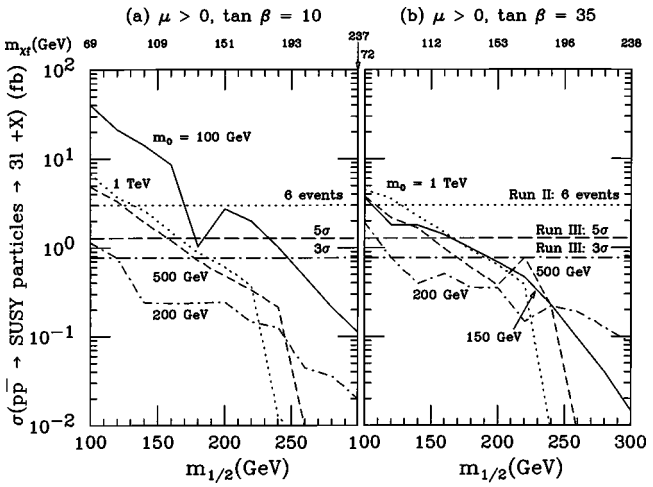

FIG. 12. Cross section of $p\bar{p}\to$SUSY particles$\to 3l+X$ with soft acceptance cuts [Eqs. (5) and (6)], versus $m_{1/2}$, at $\sqrt{s}=2$ TeV, with $\mu>0$, $m_0=100$ GeV (solid line), 200 GeV (dot-dashed line), 500 GeV (dashed line) and 1000 GeV (dotted line), for (a) $\tan\beta=10$ and (b) $\tan\beta=35$, Also noted by lines are the cross sections for (i) 6 signal events with $\mathcal{L}=2$ fb^{-1} (dotted line) and (ii) 5σ signal (dashed line) as well as 3σ signal (dot-dashed line) for $\mathcal{L}=30$ fb^{-1}. The chargino mass is given on the top horizontal scale with $m_0=500$ GeV.

SUSY sources of trileptons are included. Figure 14 shows the 99% C.L. observation contour at run II and the 5σ discovery contour as well as the 3σ observation contour at run III for $p\bar{p}\to$SUSY particles$\to 3l+X$ in the $(m_0,m_{1/2})$ parameter space for $\tan\beta=10$ and $\tan\beta=35$. We have included all SUSY sources of trileptons. For 180 GeV $\lesssim m_0 \lesssim$400 GeV and $10\lesssim\tan\beta\lesssim 40$, the χ_2^0 decays dominantly into $q\bar{q}\chi_1^0$ and in these regions it will be difficult to establish a supersymmetry signal.

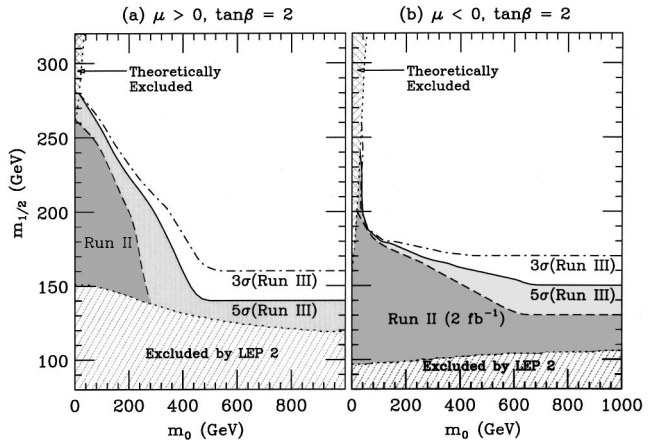

FIG. 13. Contours for 99% C.L. observation at run II and 5σ discovery as well as 3σ observation at run III in the $(m_0,m_{1/2})$ plane, for $p\bar{p}\to$SUSY particles$\to 3l+X$ at $\sqrt{s}=2$ TeV with soft acceptance cuts [Eqs. (5) and (6)], for $\tan\beta=2$, (a) $\mu>0$ and (b) $\mu<0$. All SUSY sources of trileptons are included. The shaded regions denote the parts of the parameter space excluded by (i) the theoretical requirements, or (ii) the chargino search at LEP 2.

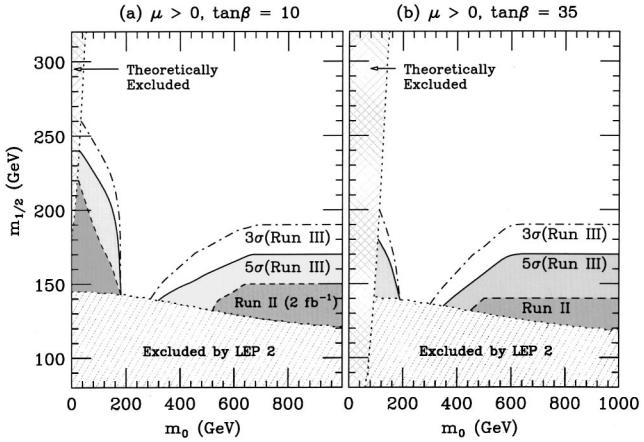

FIG. 14. The same as Fig. 13, for $\mu>0$, (a) $\tan\beta=10$ and (b) $\tan\beta=35$.

In Fig. 15, we present the contours of 99% C.L. observation at run II and 5σ discovery as well as 3σ observation at run III for $p\bar{p}\to$SUSY particles$\to 3l+X$ in the $(m_0, m_{1/2})$ plane for $\tan\beta=3$ with soft cuts A ($|M_{ll}-M_Z|>15$ GeV) and soft cuts B (18 GeV $\leqslant M_{ll}\leqslant$75 GeV). The lighter CP-even Higgs scalar mass (m_h) is sensitive to the value of $\tan\beta$. Taking $m_{1/2}=200$ GeV, $m_0=100$ GeV, $A_0=0$ and $\mu>0$, we obtain $m_h=89.5$ GeV for $\tan\beta=2$ and $m_h=99.3$ GeV for $\tan\beta=3$.

Also shown in Figs. 13, 14 and 15 are the regions that do not satisfy the following theoretical requirements: electroweak symmetry breaking (EWSB), the correct vacuum for EWSB obtained (tachyon free), and the lightest neutralino as the lightest SUSY particle (LSP). The region excluded by the $m_{\chi_1^+}\lesssim 95$ GeV limit from the chargino search [39] at LEP 2 is indicated.

We calculated cross sections for the signals and the backgrounds with tree level amplitudes. However, we expect that

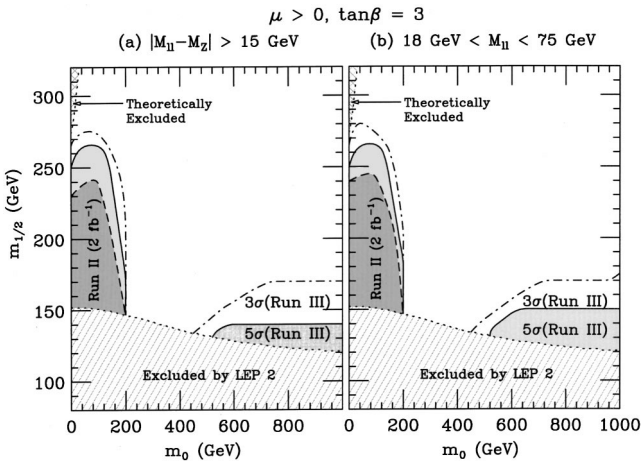

FIG. 15. The same as Fig. 13, for $\mu>0$ and $\tan\beta=3$, with (a) soft cuts A ($|M_{ll}-M_Z|>15$ GeV) and (b) soft cuts B (18 GeV $\leqslant M_{ll}\leqslant$75 GeV). The calculations in this figure are based on ISAJET 7.44 which incorporates the decay matrix elements for the charginos and the neutralinos.

our conclusions and discovery contours will be valid after QCD radiative corrections are included. Recent studies found that QCD corrections enhance the signal cross section of $p\bar{p}\to\chi_1^\pm\chi_2^0+X$ by about 10–30 % for 70 GeV $\lesssim m_{\chi_1^+}\lesssim$300 GeV [40]. QCD corrections also enhance the cross section of the dominant background $p\bar{p}\to W^*Z^*+W^*\gamma^*+X$ by about 30% [28,41].

VI. MASS RECONSTRUCTION

If the two-body decay $\chi_2^0\to\tilde{l}_R l\to l^+l^-+\chi_1^0$ is kinematically allowed and a large integrated luminosity is accumulated, it may be possible to test a predicted mass relation [42] among $m_{\chi_2^0}$, $m_{\tilde{l}_R}$ and $m_{\chi_1^0}$. To demonstrate this interesting possibility, we consider the following parameters: $m_{1/2}=200$ GeV, $m_0=100$ GeV, $A_0=0$, $\tan\beta=3$ and $\mu>0$. We evaluate masses and couplings of SUSY particles at the weak scale with renormalization group equations and obtain $m_{\chi_2^0}=143$ GeV, $m_{\tilde{e}_R}=133$ GeV, $m_{\chi_1^0}=76.0$ and $\mu=312$. The corresponding trilepton cross section after cuts $\sigma(p\bar{p}\to$SUSY particles$\to 3l+\not{E}+X)=8.6$ fb gives a promising signal with 258 events for $\mathcal{L}=30$ fb^{-1}. The $\chi_1^\pm\chi_2^0$ production contributes about 81% of the total trilepton signal.

We consider the subtracted dilepton invariant mass distribution [42] defined as

$$\left.\frac{d\sigma}{dM}\right|_{ll}=\left.\frac{d\sigma}{dM}\right|_{e^+e^-}+\left.\frac{d\sigma}{dM}\right|_{\mu^+\mu^-}-\left.\frac{d\sigma}{dM}\right|_{e^+\mu^-}-\left.\frac{d\sigma}{dM}\right|_{e^-\mu^+}. \tag{7}$$

The subtractions remove the lepton pairs with one lepton coming from $\chi_1^\pm$ and another coming from χ_2^0. This mass distribution has a sharp edge (end point) that appears near the kinematic limit for this decay sequence, i.e.,

$$M_{ll}^{\rm MAX}=M_{\chi_2^0}\sqrt{1-\frac{M_{\tilde{l}}^2}{M_{\chi_2^0}^2}}\sqrt{1-\frac{M_{\chi_1^0}^2}{M_{\tilde{l}}^2}}\approx 45\ \text{GeV}. \tag{8}$$

Figure 16 shows the subtracted invariant mass distribution for two leptons with opposite signs (l^+l^-) from $p\bar{p}\to$SUSY particles$\to 3l+X$ with $\mu>0$, $\tan\beta=3$, $m_{1/2}=200$ GeV, and $m_0=100$ GeV. This distribution may allow a test of the MSUGRA mass relations in this optimal case with a high cross section, provided that a large luminosity accumulation ($\mathcal{L}\gtrsim 10$ fb^{-1}) is obtained.

VII. CONCLUSIONS

In most of the MSUGRA parameter space, $\chi_1^\pm\chi_2^0$ production is the dominant source of trileptons. For $m_0\lesssim 150$ and $\tan\beta\gtrsim 20$, production of $\tilde{l}\tilde{\nu}$ and $\tilde{l}\tilde{l}$ can enhance the trilepton signal and may yield observable rates at run III in regions of parameter space that are otherwise inaccessible.

In some regions of MSUGRA parameter space, the $\chi_1^\pm$ and the χ_2^0 decay dominantly to final states with τ leptons.

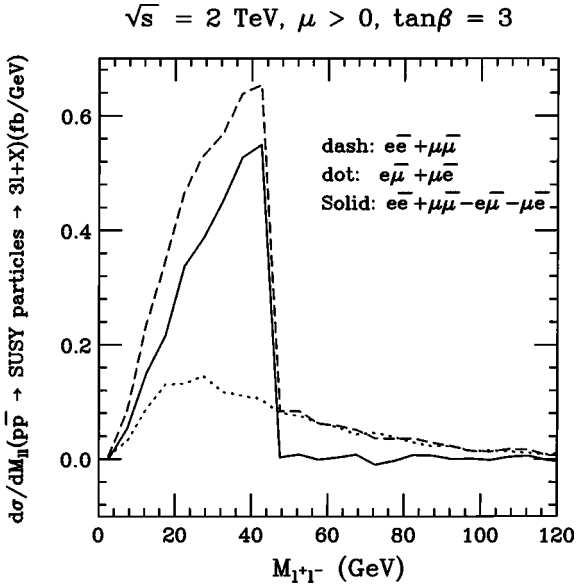

FIG. 16. The subtracted invariant mass distribution for the same flavor lepton pairs with opposite signs (l^+l^-) as defined in Eq. (7), for $p\bar{p}\rightarrow$SUSY particles$\rightarrow 3l+X$ at $\sqrt{s}=2$ TeV, with $\mu>0$, $\tan\beta=3$, $m_{1/2}=200$ GeV, and $m_0=100$ GeV.

The subsequent leptonic decays of these τ leptons contribute importantly to the trilepton signal from $\chi_1^{\pm}\chi_2^0$ associated production. With soft but realistic lepton p_T acceptance cuts, these $\tau\rightarrow l$ contributions can substantially enhance the statistical significance of the trilepton signal, compared to that with hard cuts. The branching fractions of $\chi_1^{\pm}$ and χ_2^0 decays into τ leptons are dominant when the universal scalar mass m_0 is less than about 200 GeV and/or $\tan\beta\gtrsim 40$.

The Tevatron trilepton searches are most sensitive to the region of MSUGRA parameter space with $m_0\lesssim 100$ GeV and $\tan\beta\lesssim 10$. The discovery possibilities of the upgraded Tevatron for $\mu>0$ are summarized in the following:

(i) For $m_0\sim 100$ GeV and $\tan\beta\sim 2$, the trilepton signal should be detectable at the run II if $m_{1/2}\lesssim 240$ GeV ($m_{\chi_1^{\pm}}\lesssim 177$ GeV) and at the run III if $m_{1/2}\lesssim 260$ GeV ($m_{\chi_1^{\pm}}\lesssim 195$ GeV).

(ii) For $m_0\sim 150$ GeV and $\tan\beta\sim 35$, the trilepton signal should be detectable at the run III if $m_{1/2}\lesssim 170$ GeV ($m_{\chi_1^{\pm}}\lesssim 122$ GeV).

(iii) For $m_0\gtrsim 600$ GeV and $\tan\beta\sim 35$, the trilepton signal should be detectable at the run III if $m_{1/2}\lesssim 170$ GeV ($m_{\chi_1^{\pm}}\lesssim 130$ GeV).

It might be difficult to establish a trilepton signal for 180 GeV $\lesssim m_0\lesssim 400$ GeV and $3\lesssim\tan\beta\lesssim 35$, because for these parameters $\chi_1^{\pm}$ and χ_2^0 dominantly decay into $q\bar{q}'\chi_1^0$, and the leptonic decays of χ_2^0 is suppressed. However, the important lesson is that the experiments at the Tevatron may probe a substantial region not accessible at LEP 2.

ACKNOWLEDGMENTS

V.B. thanks the Fermilab theory group for kind hospitality and support. We thank Teruki Kamon and Xerxes Tata for suggestions on the manuscript. We are grateful to Howie Baer, Regina Demina, Tao Han, Wai-Yee Keung, Jane Nachtman, Frank Paige, and Dieter Zeppenfeld for beneficial discussions. This research was supported in part by the U.S. Department of Energy under Grant No. DE-FG02-95ER40896 and in part by the University of Wisconsin Research Committee with funds granted by the Wisconsin Alumni Research Foundation.

[1] F. J. Gilman *et al.*, ''Planning for the Future of U.S. High-Energy Physics,'' HEPAP Subpanel Report, 1998.

[2] D. Amidei and R. Brock *et al.*, ''Future Electroweak Physics at the Fermilab Tevatron,'' Report of the TeV2000 Study Group, 1996.

[3] DØ Collaboration, B. Abbott *et al.*, Phys. Rev. Lett. **80**, 1591 (1998).

[4] CDF Collaboration, F. Abe *et al.*, Phys. Rev. Lett. **80**, 5275 (1998).

[5] V. Barger, C. Kao, and T.-J. Li, Phys. Lett. B **433**, 328 (1998).

[6] The SUSY trilepton signature from on-shell *W* decays was discussed in D. A. Dicus, S. Nandi, and X. Tata, Phys. Lett. **129B**, 451 (1983); A. H. Chamseddine, P. Nath, and R. Arnowitt, *ibid.* **129B**, 445 (1983); H. Baer and X. Tata, *ibid.* **155B**, 278 (1985) H. Baer, K. Hagiwara, and X. Tata, Phys. Rev. D **35**, 1598 (1987), and references therein. The importance of the trilepton signal from off-shell *W* bosons was pointed out by P. Nath and R. Arnowitt, Mod. Phys. Lett. A **2**, 331 (1987).

[7] H. Baer and X. Tata, Phys. Rev. D **47**, 2739 (1993); H. Baer, C. Kao, and X. Tata, *ibid.* **48**, 5175 (1993); H. Baer, C.-H. Chen, C. Kao, and X. Tata, *ibid.* **52**, 1565 (1995); H. Baer, C.-H. Chen, F. Paige, and X. Tata, *ibid.* **54**, 5866 (1996).

[8] R. Barbieri, F. Caravaglios, M. Frigeni, and M. L. Mangano, Nucl. Phys. **B367**, 28 (1991); J. L. Lopez, D. V. Nanopoulos, X. Wang, and A. Zichichi, Phys. Rev. D **48**, 2062 (1993); *ibid.* **52**, 142 (1995); T. Kamon, J. Lopez, P. McIntyre, and J. T. White, *ibid.* **50**, 5676 (1994); S. Mrenna, G. Kane, G. D. Kribs, and J. D. Wells, *ibid.* **53**, 1168 (1996).

[9] H. Baer, C.-H. Chen, M. Drees, F. Paige, and X. Tata, Phys. Rev. D **58**, 075008 (1998).

[10] A. H. Chamseddine, R. Arnowitt, and P. Nath, Phys. Rev. Lett. **49**, 970 (1982); L. Ibañez and G. Ross, Phys. Lett. **110B**, 215 (1982); J. Ellis, D. Nanopoulos, and K. Tamvakis, *ibid.* **121B**, 123 (1983); L. J. Hall, J. Lykken, and S. Weinberg, Phys. Rev. D **27**, 2359 (1983); L. Alvarez-Gaumé, J. Polchinski, and M. Wise, Nucl. Phys. **B121**, 495 (1983).

[11] V. Berezinskii *et al.*, Astropart. Phys. **5**, 1 (1996); P. Nath and R. Arnowitt, Phys. Rev. D **56**, 2820 (1997).

[12] K. Inoue, A. Kakuto, H. Komatsu, and H. Takeshita, Prog. Theor. Phys. **68**, 927 (1982); **71**, 413 (1984).

[13] V. Barger, M. S. Berger, and P. Ohmann, Phys. Rev. D **47**,

1093 (1993); **49**, 4908 (1994); V. Barger, M. S. Berger, P. Ohmann, and R. J. N. Phillips, Phys. Lett. B **314**, 351 (1993).

[14] J. Ellis and F. Zwirner, Nucl. Phys. **B338**, 317 (1990); G. Ross and R. G. Roberts, *ibid.* **B377**, 571 (1992); R. Arnowitt and P. Nath, Phys. Rev. Lett. **69**, 725 (1992); M. Drees and M. M. Nojiri, Nucl. Phys. **B369**, 54 (1993); S. Kelley *et al.*, *ibid.* **B398**, 3 (1993); M. Olechowski and S. Pokorski, *ibid.* **B404**, 590 (1993); G. Kane, C. Kolda, L. Roszkowski, and J. Wells, Phys. Rev. D **49**, 6173 (1994); D. J. Castaño, E. Piard, and P. Ramond, *ibid.* **49**, 4882 (1994); W. de Boer, R. Ehret, and D. Kazakov, Z. Phys. C **67**, 647 (1995); H. Baer, M. Drees, C. Kao, M. Nojiri, and X. Tata, Phys. Rev. D **50**, 2148 (1994); H. Baer, C.-H. Chen, R. Munroe, F. Paige, and X. Tata, *ibid.* **51**, 1046 (1995).

[15] E. Accomando, R. Arnowitt, and B. Dutta, Texas A&M University Report No. CTP-TAMU-43-98, hep-ph/9811300, 1998, and references therein.

[16] G. Anderson, H. Baer, C.-H. Chen, and X. Tata, Florida State University Report No. FSU-HEP-981015, hep-ph/9903370, 1999; K. Huitu, Y. Kawamura, T. Kobayashi, and K. Puolamaki, Helsinki Institute of Physics Report No. HIP-1999-13-TH, hep-ph/9903528, 1999, and references therein.

[17] H. P. Nilles, Phys. Rep. **110**, 1 (1984); H. Haber and G. Kane, *ibid.* **117**, 75 (1985).

[18] F. Paige and S. Protopopescu, in *Supercollider Physics*, edited by D. Soper (World Scientific, Singapore, 1986); H. Baer, F. Paige, S. Protopopescu, and X. Tata, in ''Proceedings of the Workshop on Physics at Current Accelerators and Supercolliders,'' Argonne National Laboratory, 1993, edited by J. Hewett, A. White and D. Zeppenfeld, hep-ph/9305342; ''ISAJET 7.40: A Monte Carlo Event Generator for $pp,\overline{p}p$, and e^+e^- Reactions,'' Brookhaven National Laboratory Report No. BNL-HET-98-39, hep-ph/9810440, 1998.

[19] H. Baer, C.-H. Chen, M. Drees, F. Paige, and X. Tata, Phys. Rev. Lett. **79**, 986 (1997).

[20] V. Barger and C. Kao, Phys. Rev. D **57**, 3131 (1998).

[21] J. F. Gunion and H. E. Haber, Phys. Rev. D **37**, 2515 (1988); R. Arnowitt and P. Nath, Phys. Lett. B **289**, 368 (1992); S. P. Martin and P. Ramond, Phys. Rev. D **48**, 5365 (1993).

[22] R. Oishi and Y. Seiya, talk presented at the Joint Working Group Meeting of Physics at Run II–Workshop on Supersymmetry/Higgs, Fermi National Accelerator Laboratory, Batavia, Illinois, 1998.

[23] J. D. Wells, Mod. Phys. Lett. A **13**, 1923 (1998).

[24] J. Lykken and K. Matchev, Phys. Rev. D (to be published), Fermilab Report No. FERMILAB-PUB-99-034-T, hep-ph/9903238, 1999.

[25] K. Matchev and D. Pierce, Phys. Rev. D **60**, 075004 (1999); Fermilab Report No. FERMILAB-PUB-99-078-T, hep-ph/9907505, 1999.

[26] H. Baer, M. Drees, F. Paige, P. Quintana, and X. Tata, Florida State University Report No. FSU-HEP-990509, hep-ph/9906233, 1999.

[27] M. S. Chanowitz and W. B. Kilgore, Phys. Lett. B **347**, 387 (1995).

[28] J. M. Campbell and R. K. Ellis, Phys. Rev. D (to be published), Fermilab Report No. FERMILAB-PUB-99-146-T, hep-ph/9905386, 1999.

[29] CLEO Collaboration, M. S. Alam *et al.*, Phys. Rev. Lett. **74**, 2885 (1995); CLEO Collaboration, S. Glenn *et al.*, contributed to the XXIX International Conference on High Energy Physics (ICHEP98), University of British Columbia, Vancouver, B.C., Canada, 1998, Report No. ICHEP98-1011, CLEO-CONF-98-17, 1998.

[30] ALEPH Collaboration, R. Barate *et al.*, Phys. Lett. B **429**, 169 (1998).

[31] P. Nath and R. Arnowitt, Phys. Lett. B **336**, 395 (1994); Phys. Rev. Lett. **74**, 4592 (1995); R. Arnowitt and P. Nath, Phys. Rev. D **54**, 2374 (1996); F. Borzumati, M. Drees, and M. Nojiri, *ibid.* **51**, 341 (1995); H. Baer and M. Brhlik, *ibid.* **55**, 3201 (1997); H. Baer, M. Brhlik, D. Castano, and X. Tata, *ibid.* **58**, 015007 (1998).

[32] H. L. Lai *et al.*, Phys. Rev. D **51**, 4763 (1995).

[33] T. Kamon, presented at the SUSY 98 Conference, Oxford, England, 1998.

[34] J. Nachtman, presented at the Joint CDF/DØ SUGRA Working Group Meeting of Physics at RUN II–Workshop on Supersymmetry/Higgs, Fermi National Accelerator Laboratory, Batavia, Illinois, 1998; J. Nachtman, D. Saltzberg, and M. Worcester, to be published in the proceedings of American Physical Society (APS) Meeting of the Division of Particles and Fields (DPF 99), Los Angeles, CA, 1999, Report No. FERMILAB-CONF-99-023-E, hep-ex/9902010, 1999.

[35] T. Stelzer and W. F. Long, computer code MADGRAPH, Comput. Phys. Commun. **81**, 357 (1994).

[36] H. Murayama, I. Watanabe and K. Hagiwara, computer code HELAS, KEK Report No. KEK-91-11, 1992.

[37] V. Barger *et al.*, report of the MSUGRA group for Physics at Run II: Workshop on Supersymmetry/Higgs, Fermilab, Batavia, Illinois, 1998.

[38] G. Jungman, M. Kamionkowski, and K. Griest, Phys. Rep. **267**, 195 (1996); M. Drees and M. Nojiri, Phys. Rev. D **47**, 376 (1993); R. Arnowitt and P. Nath, *ibid.* **54**, 2374 (1996); H. Baer and M. Brhlik, *ibid.* **53**, 597 (1996); **57**, 567 (1998); J. Ellis, T. Falk, K. Olive, and M. Srednicki, hep-ph/9905481, 1999, and references therein.

[39] ALEPH Collaboration, R. Barate *et al.*, Eur. Phys. J. C **2**, 417 (1998); CERN Report No. CERN-EP-99-014, 1999; DELPHI Collaboration, P. Abreu *et al.*, CERN Report No. CERN-EP-99-037, hep-ex/9903071, 1999; L3 Collaboration, A. Favara *et al.*, L3 note No. 2374, 1999; OPAL Collaboration, G. Abbiendi *et al.*, Eur. Phys. J. C **8**, 255 (1999); F. Cerutti *et al.*, the LEP2 SUSY working group, http://www.cern.ch/lepsusy/, LEPSUSYWG/99-03.1, 1999.

[40] T. Plehn, Ph.D. thesis, Hamburg University, Report No. DESY-THESIS-1998-024, hep-ph/9809319, 1998; W. Beenakker, M. Kramer, T. Plehn, and M. Spira, talk presented at Physics at Run II: Workshop on Supersymmetry/Higgs: Summary Meeting, Batavia, IL, 1998, hep-ph/9810290.

[41] J. Ohnemus, Phys. Rev. D **44**, 3477 (1991); **50**, 1931 (1994).

[42] A. Bartl, *et al.*, presented at 1996 DPF/DPB Summer Study on New Directions for High-Energy Physics (Snowmass 96), Snowmass, CO, 1996; I. Hinchliffe, F. E. Paige, M. D. Shapiro, J. Soderqvist, and W. Yao, Phys. Rev. D **55**, 5520 (1997).